Some Design Issues of Piezoelectric Resonating Structure for Cooling of Microelectronic Components

Maram Venkata Ramana, K.N. Seetharamu *, Indra Putra Almanar, Zaidi Mohd Ripin

School of Mechanical Engineering, University Science Malaysia
USM Engineering Campus, 14300 Nibong Tebal, Penang, Malaysia
*e-mail: knseetharamu@yahoo.com, Fax: 60-4-594-1025

Abstract

Static, model and harmonic analysis of bimetallic beam called bimorph has been performed using commercial Finite Element Analysis software package, ANSYS. The effect of damping ratio, temperature and applied electric field on the vibration characteristics of the beam has been studied. It is noted that as the damping ratio increases, the dynamic tip-deflection reduces. On increasing the temperature, first ultrasonic resonance frequency increase first then decrease. Dynamic tip-deflection increases as temperature increases. The tip-deflection is directly proportional to the applied electric field. The results are in good agreement with literature.

1. Introduction

In recent developments of science and technology, microelectronic products have become smaller and execute additional functions. This will amplify volumetric heat generation rates and surface heat fluxes in its components. Conventional methods of cooling using fan may not be suitable to dissipate heat from microelectronic products. It necessitates developing alternative method of cooling microelectronic products.

In this paper, the possibility of using Ultrasonic Flexural Waves (UFW) for cooling microelectronic components is explored. UFW can be generated by a thin bimetallic beam which can be used as a miniature fan. Piezoelectric resonating fans operate at ultrasonic frequencies provide silent operation. These fans have other advantages like small size, low power consumption and less heat generation compared to conventional fans. Piezoelectric fans are made of two thin piezoceramic layers bonded together to a central metal shim or only bonded piezoceramic layers. Ro and Loh [1] carried experiments to observe the heat transfer capability of UFW produced by piezoelectric actuation. Luis et al. [2] extensively studied the use of piezoelectric materials for controlling smart structures as sensors and actuators. Tao Wu et al. [3] simulated the behavior of piezoelectric resonating structures using FEA software. Ayo et al. [5] analyzed coupled-field finite elements to characterize piezoceramic materials subjected to temperature changes. The rapid developments in miniaturization of electronic components necessitate the above mentioned parameters to be studied, while designing the resonator structures to obtain maximum cooling effect.

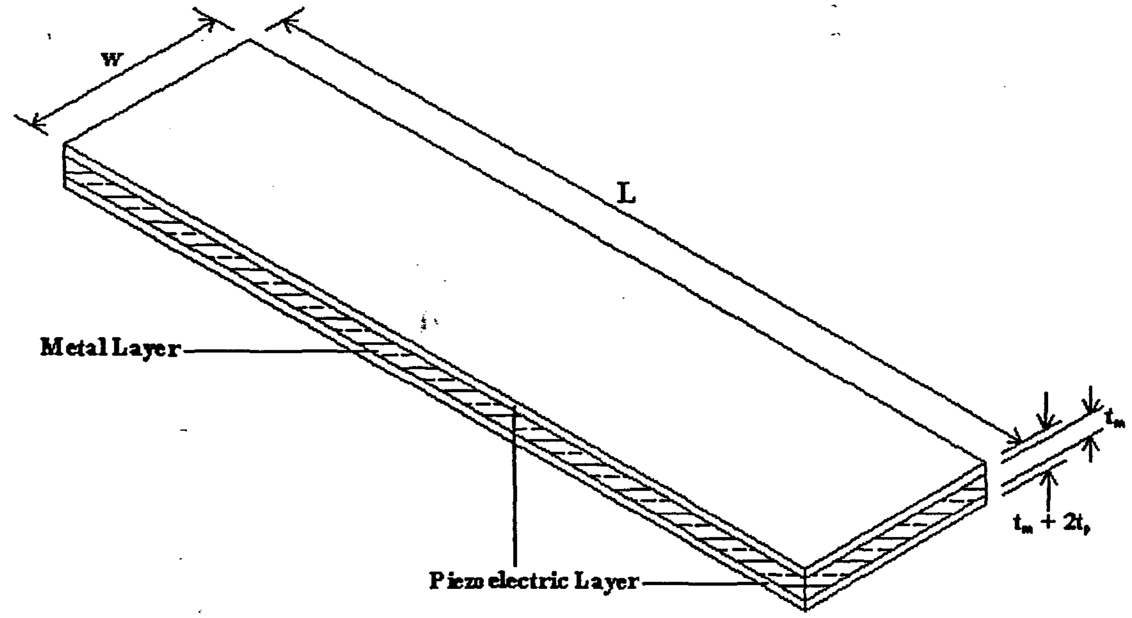

Fig. 1: Piezoceramic Bimorph Structure

2. Analysis

Numerical Simulation Method

To understand the mechanical behavior of the bimorph structure, its static, model and harmonic analysis is carried out using ANSYS. Static analysis calculates the static tip-deflection under steady loading conditions, model analysis gives the natural frequencies and mode shapes of the deformable structure. In the present simulation, model analysis was carried by reduced method with HBI (Householder-bisection-inverse iteration) algorithm. This method calculates eigenvalues and eigenvectors much faster, since it uses the concept of master degree of freedom (MDOF). In this method uses accurate stiffness matrix and estimated mass matrix. The accuracy of the solution depends on the location of MDOF. In the current study MDOF was taken along the poling direction (Z-axis). A resonator (bimorph) converts energy more effectively when it operates at resonant frequencies. Therefore, it is important to know the bimorph dynamic behavior. A full-method harmonic analysis was used to calculate the dynamic tip-deflection, which considers the full system matrices to compute the dynamic response. To obtain noise free operation of the resonator beam, the operation frequency range was set over 20 kHz. The bimorph usually consists of two thin ceramic layers bonded together. It can be noted that during vibration on of the layer expands while the other contracts. To increase the mechanical strength and stiffness a center shim is laminated between the two piezoelectric layers, as shown in Fig.1. To simulate the bimorph, the piezoelectric actuator patches were constructed using 3D coupled-field solid elements SOLID5 and the middle brass shim was modeled by SOLID45. The element edge lengths on surface boundaries of 0.5, 0.4, 0.3 and 0.2 mm were tested. Little variation in the parameters of interest, i.e., resonance frequencies and dynamic displacements, was observed between the last two smallest grid solutions, therefore the final meshing edge length was fixed at 0.3 mm to guarantee reasonable accuracy and speed. The fixed–free boundary condition was applied by constraining the nodal displacements in *x*, *y* and *z* directions at one end of the beam. To simulate the electrode surfaces of the bimorph actuator, the same level of nodal electrical potential was prescribed at the nodes on the surfaces.

Piezoelectric Material Data

Manufacturers of piezoelectric materials do not issue the material properties in a format that can be directly fed to ANSYS. This data must be transformed to necessary material matrices as a piezoelectric material input. ANSYS requires a dielectric matrix[ε], a piezoelectric matrix[e] and either a compliance matrix[d] or a stiffness matrix[c]. The dielectric matrix[ε] is 3X3 diagonal matrix which defines the electrical permittivity. This data can be entered into ANSYS as an orthotropic material property with the labels PERZ, PERY and PERZ. The piezoelectric matrix, [e], defines the electric field to stress and it is of the form 6X3 matrix and the data is entered into ANSYS as a material data table of PIEZ. The stiffness data can be fed to ANSYS in the form of elastic modulus and Poisson's but it is more common to practice in coupled field analysis to define either compliance matrix[s] or stiffness matrix[c].It is of the form 6X6 symmetric matrix, data is entered into ANSYS as a material data table of ANEL. Typical manufactures supplied material data as follows:

$$S=\begin{bmatrix} s_{11} & s_{12} & s_{13} & 0 & 0 & 0 \\ s_{12} & s_{11} & s_{13} & 0 & 0 & 0 \\ s_{13} & s_{13} & s_{33} & 0 & 0 & 0 \\ 0 & 0 & 0 & 2(s_{11}-s_{12}) & 0 & 0 \\ 0 & 0 & 0 & & s_{55} & 0 \\ 0 & 0 & 0 & 0 & 0 & s_{55} \end{bmatrix}$$

$$d=\begin{bmatrix} 0 & 0 & 0 & 0 & 0 & d_{15} \\ 0 & 0 & 0 & 0 & d_{15} & 0 \\ d_{31} & d_{31} & d_{33} & 0 & 0 & 0 \end{bmatrix}$$

$$\varepsilon=\begin{bmatrix} \varepsilon_{11} & 0 & 0 \\ 0 & \varepsilon_{22} & 0 \\ 0 & 0 & \varepsilon_{33} \end{bmatrix}$$

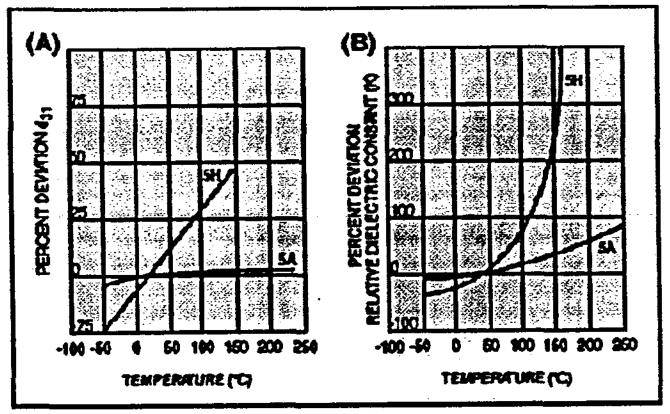

Fig. 2: Temperature dependent material properties for PSI-5H and PSI-5A

Temperature Dependence of Piezoelectric Material Properties

Piezoelectric materials show significant changes in their material property as a function of temperature. It can be observed from the Fig.2 that, at a temperature of 150°C d31, increases by about 45% compared to that at room temperature piezoelectric strain coefficient, d31 of temperature-sensitive material PSI-5H. It can be further observed that the increase only 5% for temperature-insensitive PSI-5A. On the other hand, the relative dielectric constant K, can be seen to increase as much as 275% at 150°C for PSI-5H and for PSI-5A around 45% increase. In the present work, commercial piezoelectric material (PSI-5H) from Piezo Systems Inc., [6] was used. The thickness of the metal shim is 0.127mm and each piezoceramic layer thickness is 0.191mm.

3. Verification of Numerical Simulation

Static and model analysis results are verified with analytical method for the model shown in Fig.1. As the bimorph is made of metal and piezoceramic layer have different elastic moduli, transformed cross section method of composite beam is selected to determine the static tip deflection and fundamental resonance frequency. The analytical expression for static tip deflection and fundamental resonance frequency are given as [3].

$$\delta=\frac{3L^2}{2t}\frac{(1+B)(1+2B)}{AB^3+3B^2+3B+1}d_{31}E_3 \qquad (5)$$

$$f_r=\frac{3.52t}{4\pi L^2}\sqrt{\frac{E_p}{3\rho_p}}\left[\frac{1+3(1+2B)^2+4AB^3}{4(1+B)^2(BC+1)}\right]^{1/2} \qquad (6)$$

Where:

δ = static tip deflection

f_r = fundamental resonance frequency

d_{31} = piezoelectric constant

E_3 = electric field strength

ρ_p = density of piezoelectric layer

E_p = Young's modulus of piezoelectric layer

ρ_m = density of metal

E_m = Young's modulus of metal

t_m = thickness of metal

t_p = thickness of piezoelectric

L = length of the beam

t = total thickness of the bimorph

$= t_m + 2t_p$

$$A=\frac{E_m}{E_p},\quad B=\frac{t_m}{2t_p},\quad C=\frac{\rho_m}{\rho_p}$$

A bimorph of an 8 mm × 2 mm metal shim bonded with two same-size ceramic layers was used to compare numerical simulation results with the analytical ones that are obtained using equations (5) and (6). The static response of the bimorph was determined by applying an electrical field of 200 V mm^{-1} on both PZT patches, keeping the total thickness constant at t = 0.4 mm. The properties of PZT ceramic and two alternative metal materials are listed in table 1[3].

Table 1: Material Properties

Materials	d31× 10^{-12} (m/V)	Young's Modulus ×10^{10} (N m^{-2})	Density (kg m^{-3})	Poisson's ratio
PZT ceramic	-190	6.6	7800	0.31
Brass	--	11.0	8800	0.35
Alumni.	--	6.5	2992	0.35

Table 2: Material properties of PSI-5H at room temperature

d_{31}	-274 X 10^{-12} m/V
d_{33}	593 X 10^{-12} m/V
d_{15}	720 X 10^{-12} m/V
S_{11}	16.4 X 10^{-12} m2/N
S_{12}	-4.7 X 10^{-12} m2/N
S_{13}	-7.5 X 10^{-12} m2/N
S_{33}	20.8 X 10^{-12} m2/N
S_{55}	43 X 10^{-12} m2/N
K_{11}	3130
K_{33}	3400
ε_0	8.85 f/m
Density	7750 kg/m^3

To validate the simulation results with those obtained from analytical relations are plot tip deflection δ versus thickness ratio B and first fundamental resonance frequency versus thickness ratio B for brass and aluminum are shown in Fig. 3 and Fig. 4 respectively.

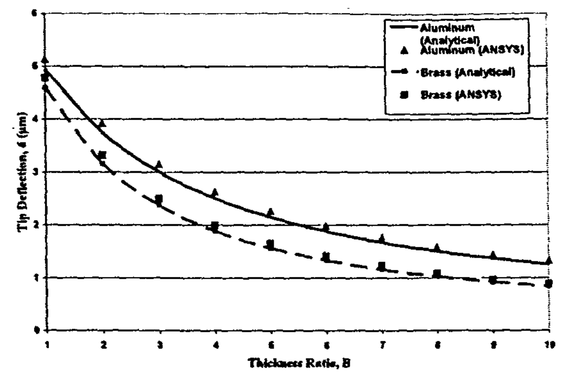

Fig. 3: Static Tip Deflection Vs Thickness Ratio.

The good agreement between the finite element simulation and the analytical solution gives confidence that the present computer simulation method is sufficiently accurate to analyze more complicated piezoelectric structures.

4. Results and Discussion

Effect of damping ratio

A constant damping ratio of 0 %, 1 % and 2 % assumed for all the frequencies for the harmonic analysis. The data from the table 1 is used for the analysis. It can be observed from Fig.6 that the peak amplitude for each case is different and it is also observed that by increasing the damping ratio the peak amplitude decreases. A damping ratio 1% is considered for all further analysis.

Effect of thickness ratio on tip-deflection

As shown from the Fig.3, the effect of an elastic layer on tip deflection can be obtained by plotting tip deflection δ versus thickness ratio B for two elastic materials.

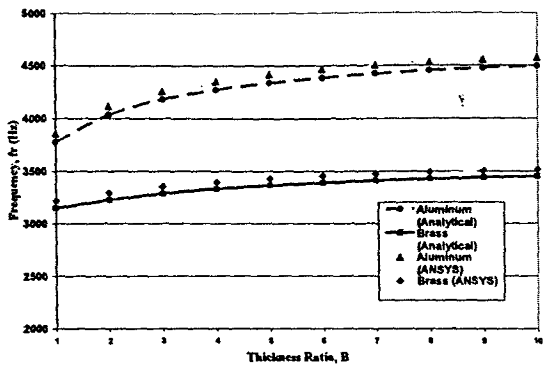

Fig. 4: Resonance Frequency Vs Thickness Ratio.

As the metal layer thickness increases and the PZT layer decreases (B increases) tip deflection will decrease. It can be further observed from Fig. 3 that, the tip-deflection fro any given thickness, is more for aluminum than that of brass.

Effect of thickness ratio on first resonance frequency

Modal analysis is used to obtain the mode shapes. Fundamental resonance frequency versus thickness ratio B for brass and aluminum is shown in Fig. 4. It can be seen that the use of an aluminum metal layer leads to much higher resonance frequency than brass because of its lower density. The increased thickness of metal layer will increase the stiffness of the entire bimorph causing the resonance frequency to increase.

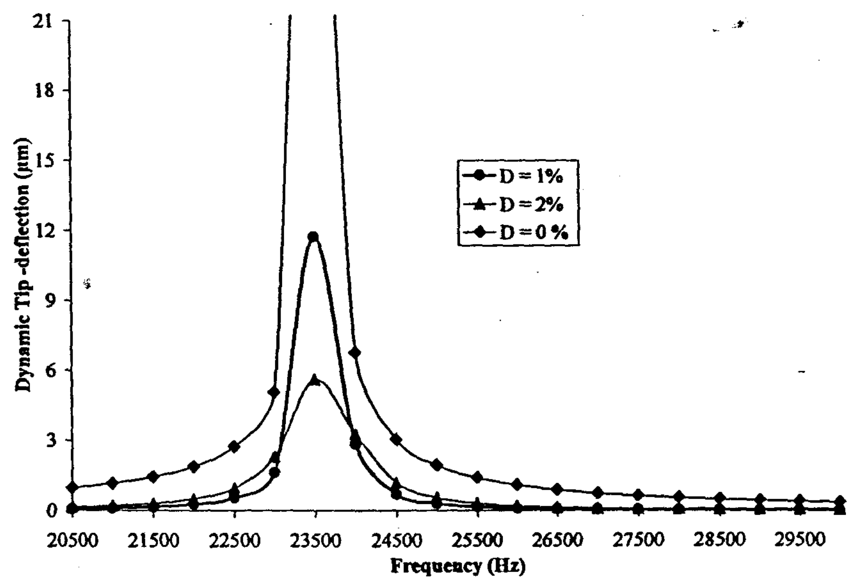

Fig. 5: Harmonic response for different damping ratios

Effect of bimorph length

In order to analyze the effect of bimorph length on vibration characteristics we considered five configurations 6mm, 7mm, 8mm, 9mm and 10mm. Constant width of 2mm was taken for all the five cases. From the table 3 it is evident that as bimorph length increases its fundamental resonance frequency decreases. Since longer beam easier to vibrate and results lower resonance frequencies.

Table 3. Resonance frequencies

Lengt h (mm)	1st mode resonance frequency (Hz)	2nd mode resonance frequency (Hz)	3rd mode resonance frequency (Hz)
6	6546	39953	109838
7	4804	29517	81399
8	36735	22681	62868
9	2900	17965	49884
10	2346	14566	40573

The surface velocity of the bimorph depends on the cumulative effect of first ultrasonic resonance frequency and corresponding dynamic tip-deflection. It can be observed from table. 4 that the 7mm length bimorph yields highest surface velocity which makes it most preferable to the cooling application.

Effect of temperature on tip-deflection

To simulate the temperature effects, we obtained required material matrices by scaling the room temperature properties from table. 2 and percentage deviation from Fig.2. In this study 7mm X 2mm bimorph was considered. It was observed that dynamic tip-deflection is increase with increase in temperature as is evident from Fig.7

Table. 4 Surface velocities for different bimorph lengths

Lengt h (mm)	First Ultrasonic Resonance frequency(f=Hz)	Dynamic tip-deflection (A=µm)	Surface velocity (m/s)
6	39953	9.00	2.26
7	29517	13.8	2.56
8	22681	15.0	2.14
9	49884	5.20	1.63
10	40573	6.30	1.61

Effect of temperature on first ultrasonic resonance frequency

It is observed from the Fig.7 that first resonance frequency initially, increases with the increase in temperature, reaches a maximum value at 0°C and there after decreases continuously with increase in temperature.

Effect of Electric field applied

As seen from the Fig.8 the static tip-deflection is directly proportional to electric field applied. The predicted values are closely agreed with the analytical values from equation (5). There is no effect of resonance frequency on the temperature applied, which satisfies the relation (6).

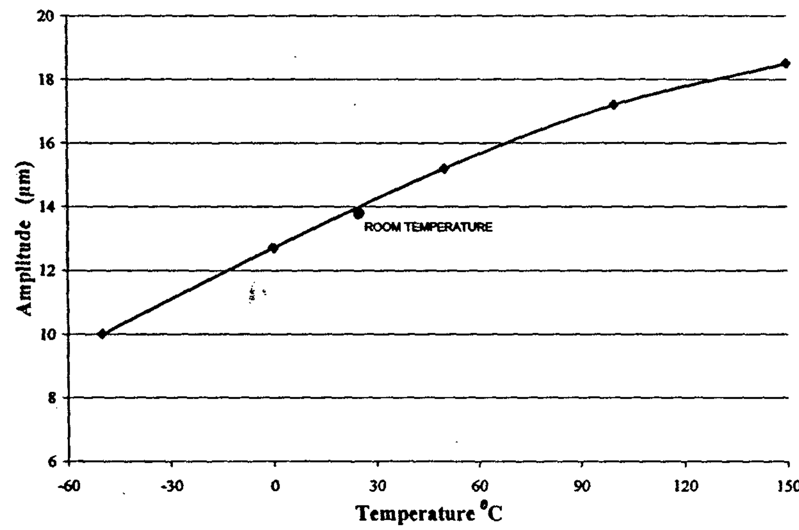

Fig. 6: Harmonic response at different damping ratio

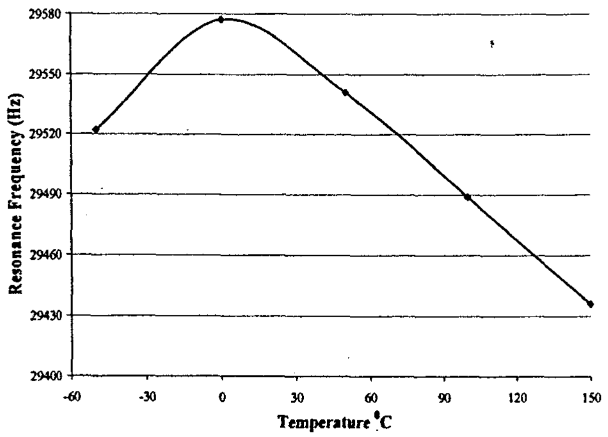

Fig. 7: First ultrasonic resonance frequency Vs Temperature

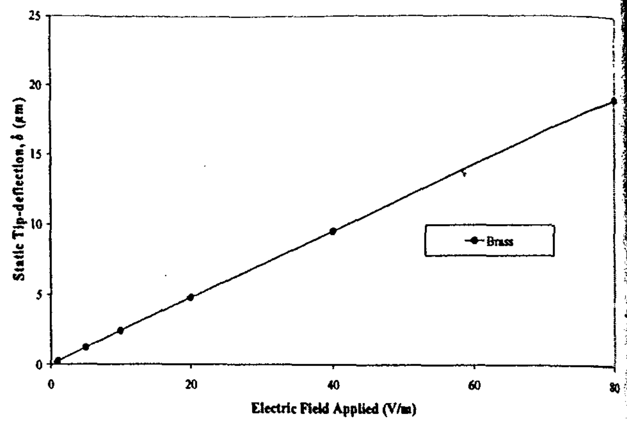

Fig. 8: Static tip-deflection Vs Electric field applied

5. Conclusion:

The modeling of a piezoelectric resonating structure was carried out using Finite Element Analysis software, ANSYS. From the analysis, it can be seen that with the increase in thickness ratio, the tip-deflection will increase but resonance frequency decreases. In choosing a piezoceramic material for cooling effect, a material with higher piezoelectric matrix[d], lower elasticity stiffness matrix [c] is desired. The 7mm length bimorph gives higher surface velocity as compared to other bimorph configurations. The deflection of the bimorph greatly influences the temperature behavior of the piezoelectric strain coefficient, d_{31}. The electric field applied will only affect the tip-deflection.

6. Acknowledgements

Authors would like to thank School of Mechanical Engineering, Universiti Sains Malaysia for providing the necessary financial support from the FRGS grant No. 6070010.

7. References

1. Ro P I and Loh B G, "Feasibility of Using Flexural Waves as a Cooling Mechanism", *IEEE Transactions on Industrial Electronics*, Vol.48, No.1, pp 143-149. February, 2001
2. Crawly E F and Luis D J, "Use of Piezoelectric Actuator as Elements of Intelligent Structures", *AIAA J.25*, Pages 1373-1385, 1987
3. Tao Wu, Paul I Ro, Angus I Kingon and James F Mulling, "Piezoelectric Resonating Structures for Microelectronic Cooling", *Institute of Physics Publishing, Smart Materials and Structures*, 12 , pages 181-187,2003.
4. Loh B G, Hyun S, Ro P I and Kleinstreuer C, "Acoustic Streaming Induced by Ultrasonic Flexural Vibrations and Associated Enhancement of convective heat transfer" *J. Acoust. Soc. Am.*, 111, 875-883,2002
5. Ayo O A,Malluck J F,Zhibo T, "Using Coupled-Field Finite Elements to Characterize Piezoceramic Materials" Sensors online, June 1998.
6. Piezo Systems Inc., Product Catalogue, Cambridge, MA
7. Philipp Burmann, Arvind Raman and Suresh V.Garimella "Dynamics and Topology Optimization of Piezoelectric Fans" IEEE Transactions on Components and Packaging Technologies, Vol. 25, No.4, 592-600, December 2003.
8. JohnsonD.H, EriePS and PalD "Simulation of an Ultrasonic Piezoelectric Transducer" Online at www.ohiocae.com
9. Lin M W and Abatan A O " Application of commercial finite element codes for the analysis of induced strainactuated structures" J.Intell .Mater.Syst.Struc.5,869-875,1994.
10. ANSYS Theory manual (www.ansys.com)

11. Krishnamoorthy C S, Indian Institute of Technology, Madras, Finite Element Analysis,Theory and Programing, Tata McGraw-Hill Publishing Company Limited, New Delhi,1987

Three dimensional Conjugate Heat Transfer Analysis of Single Chip Mounted on PCB

BABBKT
30375

Maram Venkata Ramana
School of Mechanical Engineering
Universiti Sains Malaysia
14300, Nibong Tebal, Penang, Malaysia
Email: maram_ven@yahoo.com

Indra Putra Almanar
School of Mechanical Engineering
Universiti Sains Malaysia
14300, Nibong Tebal, Penang, Malaysia
Email: meinput@eng.usm.my

M.Z. Abdullah
School of Mechanical Engineering
Universiti Sains Malaysia
14300, Nibong Tebal, Penang, Malaysia
Email: knseetharamu@yahoo.com

Zaidi Mohd.Ripin
School of Mechanical Engineering
Universiti Sains Malaysia
14300, Nibong Tebal, Penang, Malaysia
Email: mezaidi@eng.usm.my

K.N. Seetharamu
M S Ramaiah School of Advanced Studies
New BEL Road, Bangalore 560 054, India
Email: knseetharamu@yahoo.com

Abstract

Piezoelectric fans are investigated as alternative method of cooling micro electronic components. In the present study, five types of piezoelectric fans with constant width are considered. Three dimensional finite element analysis is carried out to calculate air stream velocities generated by the fans using commercial FEM software package ANSYS. Three dimensional conjugate heat transfer analysis of single chip mounted on printed circuit board is carried out using a finite volume based CFD code, FLUENT. Investigations on some parameters of interest like gap between the fan and chip, chip power for all five cases are studied. The predicted results are presented in terms of temperature distribution of the chip, variation of the heat transfer coefficient along the chip. It is observed that piezoelectric fan with five blades gives the maximum average velocity. With applied electric voltage 200 V/mm, these fans are more effective for chips dissipating less than 0.5W power.

Keywords: Piezoelectric fans, Conjugate heat transfer analysis, Microelectronic Cooling.

1. Introduction

Thermal management in future electronic components is crucial for rapid development of the electronic industry. To increase the performance as well as reliability of the electronic components a steady and low operating temperature is a must. Traditional methods of cooling using heat sink and fan combinations are obstacle to miniaturisation of the modern electronic devices. Piezoelectric fans are considered as promising substitute to augment convection currents where space, power and noise are primary concern. These fans first appeared in early seventies. Toda [1] verified airflow and cooling capabilities generated by an eight layered cantilever piezofan. Yoo et al. [2] built-up different types of piezofans. These fans achieved air velocity of the order 3m/s at tip-deflection 3.55 cm. Ro et al and Wu et al [3,4] demonstrated the feasibility of an air stream generated by acoustic streaming on a relatively large beam actuator as cooling mechanism for micro electronic components. Buermann et al. [5] conducted an optimization study of a piezoelectric fan with two symmetrically placed piezoelectric patches. These studies clearly showed that piezoelectric fans are producing jet like airflow for cooling of electronic components. There are several studies on electronic components cooling. Conjugate heat transfer from a surface-mounted block ($31\times31\times7$ mm^3) to forced convective airflow (1-7 ms^{-1}) in a parallel-plate channel is studied experimentally and analytically by Nakayama and Park [6]. Hung and Fu [7] developed a two-dimensional model for numerical prediction of viscous laminar flow, mixed convection and conjugate heat transfer between parallel plates with uniform block heat sources and with openings on the integrated circuit board. Quadir et al. [8] reported a three-dimensional analysis of the heat and fluid flow over a single 84 pins PLCC package mounted on a Printed Circuit Board (PCB) along the direction of flow. However, the winning application of piezoelectric fans for on-chip cooling is still challenging.

In this paper, to understand the cooling effect produced by the piezoelectric bimorph structures, a three dimensional conjugate heat transfer analysis is carried out. Five types of piezoelectric fans with constant width of 10mm are considered. These configurations are shown in Fig.1. Three dimensional finite element analysis is carried out to calculate air stream velocities generated by the fans using commercial FEM software package ANSYS. Then three dimensional conjugate heat transfer analysis of single chip mounted on printed circuit board is carried out using a finite volume based CFD code, FLUENT.

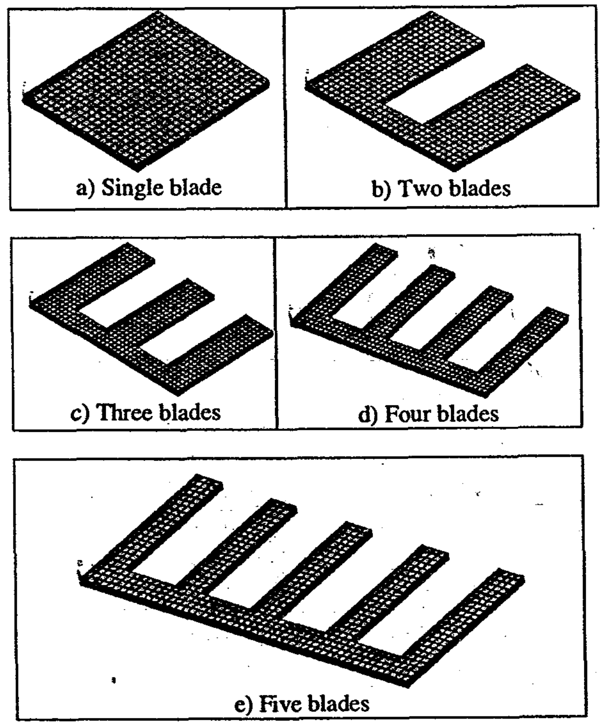

Fig.1. Different configurations of the bimorph

2. Analysis

2.1 Numerical Simulation Using ANSYS:

To determine the amount of air generated, it is necessary to find the vibration characteristics of the bimorph structure. There are many reports available on analytical relation to calculate natural frequency and static tip-deflection for simple bimorph structures [3], but it is very difficult to formulate the analytical expressions for each and every structure. In this work, vibration characteristics are simulated using the commercial Finite Element Method software package ANSYS 6.0.

Modal and harmonic analysis, are performed in the numerical simulation by the commercial finite element method software package ANSYS. Modal analysis is used to calculate the resonance frequencies and mode shapes of mechanical systems. Modal analysis was carried by using the reduced method. The reduced method uses the Householder-Bisection-Inverse iteration (HBI) algorithm to calculate solution of the equation of motion of a deformable system. Reduced method with HBI algorithm is relatively fast because it uses the master DOF. The full-method harmonic analysis was used to calculate the dynamic behaviour of the structure, uses the full system matrices to calculate the harmonic response. To attain silent operation of resonator beam, operation frequency range was set over 20 kHz. To simulate the bimorph, the piezoelectric actuator patches are constructed using 3D coupled-field solid elements SOLID5 and the middle brass shim was modeled by SOLID45. All other dimensions for the simulation of bimorph thickness and material properties are same as that used by Maram et al. [9]. The element edge lengths on surface boundaries of 0.5, 0.4, 0.3 and 0.2 mm were tested. Little variation in the parameters of interest, i.e., resonance frequencies and dynamic displacements, is observed between the last two smallest grid solutions, so the final meshing edge length was 0.3 mm to guarantee reasonable accuracy and speed. The fixed–free boundary condition was applied by constraining the nodal displacements in *x*, *y* and *z* directions at one end of the beam. To simulate the electrode surfaces of the bimorph actuator, the same level of nodal electrical potential is prescribed at the nodes on the surfaces.

2.2 Numerical Simulation Using FLUENT:

The finite volume method based computational fluid dynamics software package FLUENT 5.2 is used for the numerical simulation. Double precision, three-dimensional solver is used with default convergence criteria for continuity, x, y and z velocities. SIMPLE algorithm was used for the pressure correction. The basic equations describing the flow of fluid are conservation of mass, conservation of momentum and conservation of energy. FLUENT normally solves the governing conservation equations using Cartesian spatial coordinates and velocity components. As the piezoelectric fan generates jet like airflow, second order upwind discretization scheme is used for momentum and energy. Second order discretization scheme is used for pressure.

From the results obtained from the structural analysis, air velocities developed in each case is less than or equal to 2 m/s (Refer Table.1). The Reynolds number is calculated based on these velocities are below 12300. Thus flow field generated in each case fall under the laminar region.

2.3 Modeling

The flow domain used in this simulation consists of a rectangular enclosure. It consists of whole computational domain with a motherboard in it and a chip attached on top of the motherboard. The isometric view is shown in Fig.2. Table.2 gives several critical distances. All other dimensions for the simulation setup are similar to those used by Quadir et al. [8].

All surfaces of the enclosure are insulated and no-slip boundary conditions are applied at all solid surfaces, except inlet and exit. At the front surface, to represent piezoelectric fan corresponding opening are

provided for each case. Fig.2 gives the isomeric view for the case 2 (two blades). At back surface is treated as outlet. As for the motherboard and package, no-slip boundary conditions are applied at the surfaces. To take conjugate effect into consideration, coupled option is selected for all surfaces exposed to the fluid. A lumped model is used to model the packages. Thus, the properties of the packages are uniform throughout. The model used in this simulation consists of a flow domain that encompasses the motherboard in it and one Plastic Leaded Chip Carriers (PLCC) on top of the motherboard. The dimensions of the components are enclosure 50 X 10 X 10cm^3, chip 2.72 X 0.03 X 2.72 cm^3, motherboard 33 X 0.38 X 8 cm^3.

2.4 Grid Generation

In this simulation, the computational domain is meshed with 8 node quadrilateral elements. There are a total of 92004 elements and 102120 nodes are used to mesh model. This particular grid size is chosen as it offered the best compromise between a coarse grid and a dense grid especially in the J-direction. Smaller number of node points would result in irregularly spaced cells between the denser critical sections with the rest of the flow domain. On the other hand, the computing capacity of the workstation becomes the limiting factor for the inability to assign higher node points. The completed numerical model with uneven grid distribution is shown in Fig. 3.

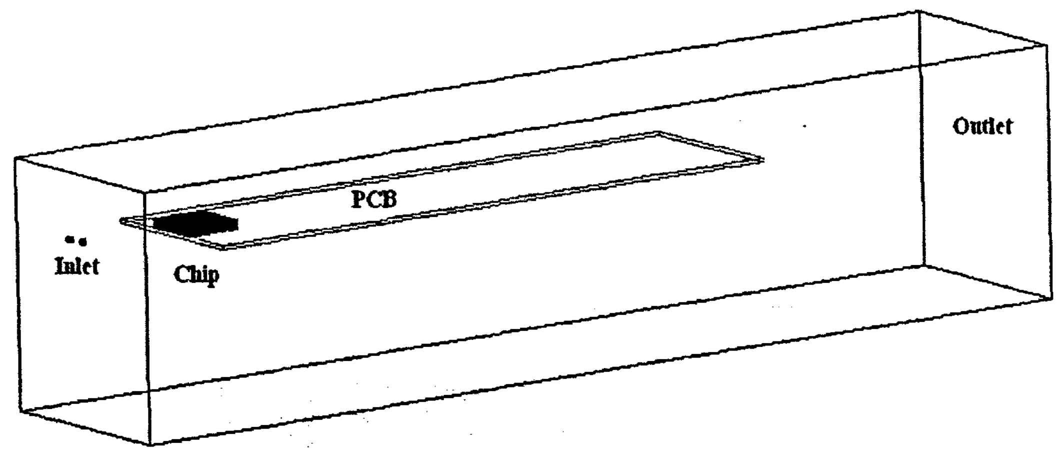

Fig.2 Isometric view of the flow domain for the Case 2
(To simulate the bimorph structure with two blades)

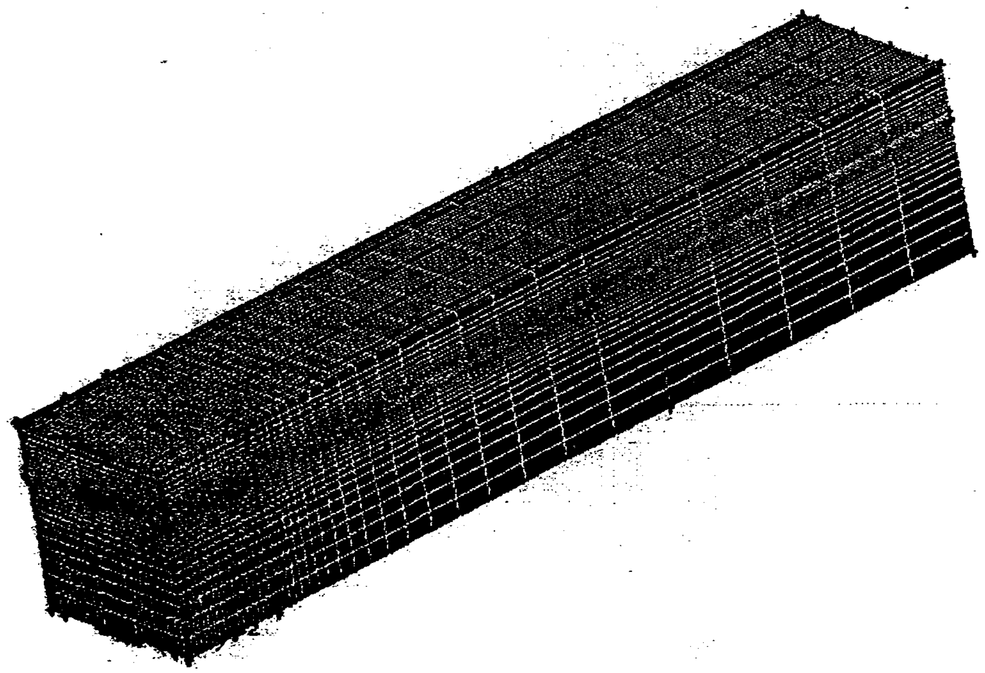

Fig.3 Flow domain considered for the CFD simulation.

3. Results and Discussions

3.1. Numerical Model Validation

The structural analysis methodology applied is validated with the results published by Ro et al [4] and Maram et al. [9]. Numerical simulation considered for conjugate heat transfer analysis, using FLUENT is compared with Quadir et al. [8]. Then the same methodology is applied to the present simulation.

3.2.1Characteristic Surface Velocity

A typical modal analysis result for bimorph with two blades is shown in Fig.4. Dynamic tip-deflection obtained from the harmonic response of the bimorph with three blades is shown in Fig.5. From the modal analysis it is found that maximum displacement occurs at tip for cantilever beams. So, the characteristic surface velocity generated is defined as the product of the first ultrasonic resonance frequency and corresponding dynamic tip-deflection.

$$V = 2 * \pi * A * f \qquad (1)$$

Where A = dynamic tip-deflection
f = first ultrasonic resonance frequency

The comparative characteristic velocities observed for the five Cases considered are listed in Table 1.

Table.1 Comparative air velocities produced by five bimorph configurations

Fan Type	Limb	Air Velocity (m/s)
Case 1 (One blade)	1	1.393
Case 2 (Two blades)	2.1	1.079
	2.2	1.079
Case 3 (Three blades)	3.1	1. 509
	3.2	1. 537
	3.3	1. 509
Case 4 (Four blades)	4.1	1.392
	4.2	1.661
	4.3	1.661
	4.4	1.392
Case 5 (Five blades)	5.1	1.621
	5.2	1.918
	5.3	2.070
	5.4	1.918
	5.5	1.621

Air stream velocities generated are different in each case. It is observed from the Table.1, that average velocity generated is high when bimorph structure is vibrating with five blades. The average velocity obtained from Case 3 and Case 4 is almost same and higher than the other two cases. It is shown that Case2 gives the lowest average velocity. From this analysis, to achieve maximum velocity bimorph with more than two blades configuration is best for cooling of microelectronic components.

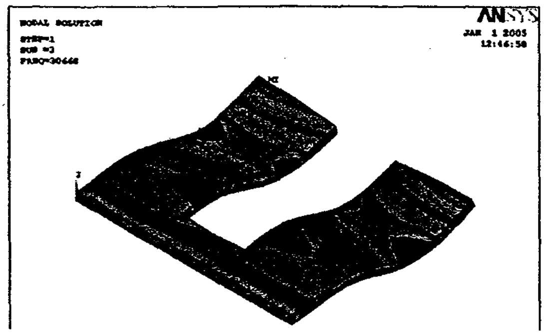

Fig.4 First Ultrasonic resonance frequency of bimorph with two blades

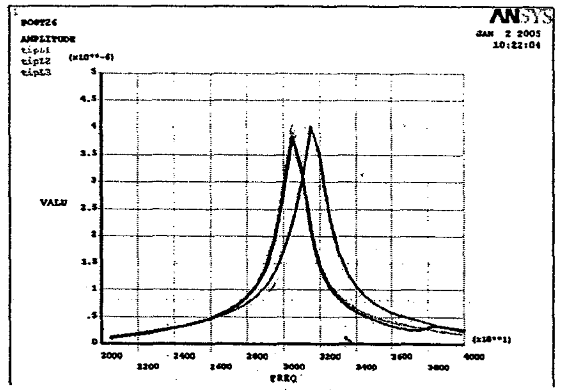

Fig.5 Dynamic tip-deflection of bimorph with three blades

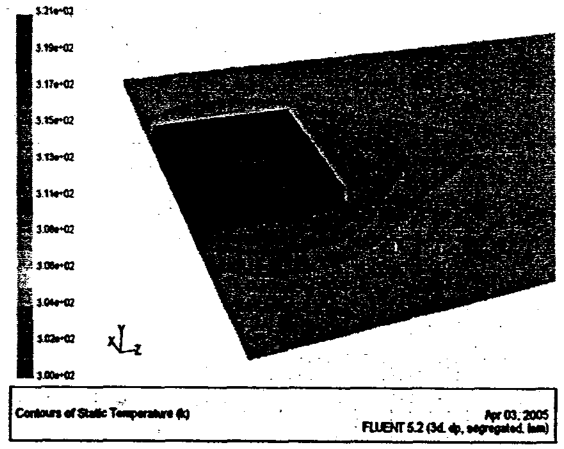

Fig. 6 Contours of static temperature for the model 3 when Gap 10mm and Power 0.25W

3.2.2 Effect of Gap on Chip Temperature:

In the present analysis, chip dissipating 0.25W, 0.5W and 1.0W are considered. The gap between inlet and chip is also analyzed for three conditions (10mm, 20mm and 30mm). There are a total of 45 cases. Static temperature distribution of a typical case is shown in the Fig.6. Similar type of behaviour is observed in all cases. The list of predicted chip temperatures are presented in Table.2

Table.2 List of simulated chip temperature from the analysis

Gap = 10 mm	Temperature (°C)		
Case	0.25W	0.5W	1.0W
1	48.7	65.3	118.0
2	54.2	71.5	136.0
3	48.0	69.0	111.0
4	48.2	69.3	112.0
5	45.4	63.8	101.0
Gap = 20 mm	Temperature (°C)		
Case	0.25W	0.5W	1.0W
1	50.6	74.2	121.0
2	54.4	81.8	137.0
3	50.0	72.9	119.0
4	48.8	69.7	113.0
5	45.7	64.5	102.0
Gap = 30 mm	Temperature (°C)		
Case	0.25W	0.5W	1.0W
1	51.8	76.6	126.2
2	55.2	84.4	142.0
3	49.3	71.7	116.4
4	51.6	76.2	125.0
5	46.3	65.6	104.2

From the above Table.2, it is evident that Case5, (bimorph structure with five blades) gives the highest cooling effect as compared to other cases for the same chip power and gap between inlet and chip. It is also noted that as the gap between inlet to chip increases cooling performance of the structure is decreasing. Temperatures observed for chip dissipating 1.0W power are above 100°C. This means with the input voltage of 200 V/mm, the bimorph configurations considered are able to work below chip dissipating 0.5Watts. In other wards to give best solutions to the chip dissipating more than 0.5 Watts, change design criteria of the bimorph structure. This can be achieved in several ways i.e. alter the thickness ratio of the bimorph, change the piezoceramic layer, introduce the distributed piezoceramic layers, change material for centre shim and increase input voltage etc.

3.2.3 Heat Transfer Coefficient Variation:

From the predicted simulation results, it is evident that the heat transfer coefficient is higher at the leading edges of the packages for all 45 cases. Fig.12 and Fig.13 plotted front surface heat transfer coefficient vs. chip length. The average heat transfer coefficient from the above cases is listed in Table.3. Highest heat transfer coefficient is achieved for Case 3 but high cooling is obtained from the Case 5 (ref. Table.3). This is mainly because of the amount of air injected is higher in the Case 5 and also air inputs are equally spread on the chip front surface. Similar type of behaviour is observed with other cases. It is concluded that Case 5 i.e. bimorph structure with 5 blades gives the high cooling performance. The predicted contours of heat transfer coefficient distribution for chip and PCB is shown in following figures from Fig.7 to Fig. 8.

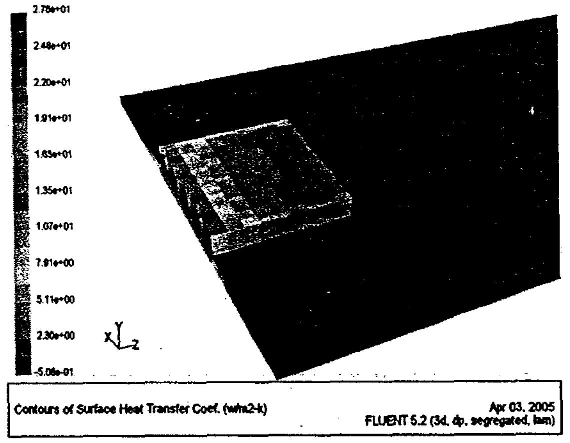

Fig.7 Contours of surface heat transfer coefficient for Case 5 when gap 20mm and power 0.5W

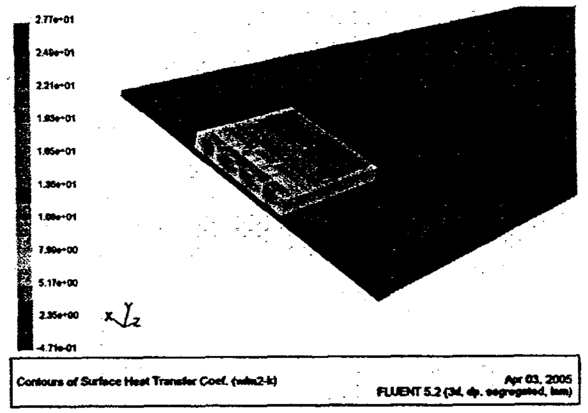

Fig.8 Contours of surface heat transfer coefficient for Case 4 when gap 20mm and power 0.5W

4. Conclusions

A three dimensional conjugate heat transfer analysis single chip mounted on a printed circuit board is carried out using an available commercial CFD code, FLUENT. It is observed that piezoelectric fan with five blades gives the maximum average velocity and hence produces more cooling effect. With the application of 200 V/mm, these fans are more effective for chips dissipating less than 0.5W power. There is no significant change in the top surface average heat transfer coefficient with the variation of chip package power. The predicted heat transfer coefficient is very high at front surface and goes on reducing to minimum value at the trailing edge for all cases.

Table. 3 Average Surface Heat Transfer Coefficients (S.H.T.C) when gap = 20 mm and chip power = 0.5W

Case	S.H.T.C (W/m^2K)
Case 1	21.96
Case 2	19.47
Case 3	23.93
Case 4	22.88
Case 5	23.72

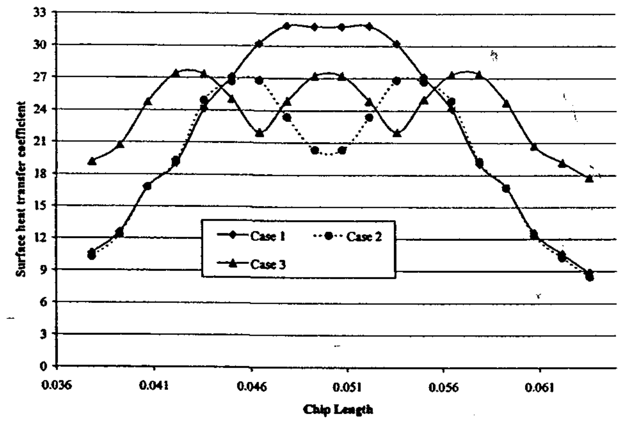

Fig.10 Front surface heat transfer coefficient distribution when gap = 20 mm and chip power = 0.5W

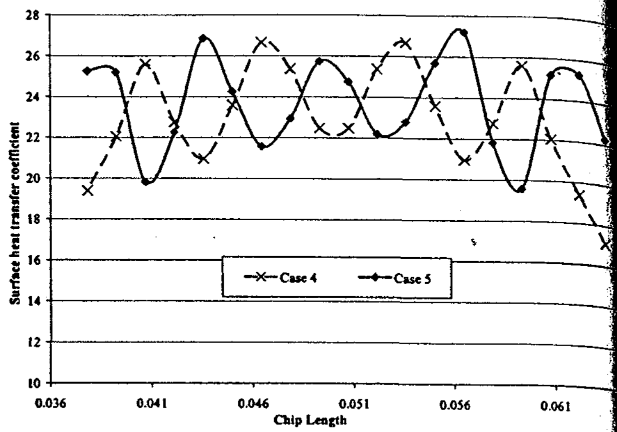

Fig. 11 Front surface heat transfer coefficient distribution when gap = 20 mm and chip power = 0.5W

5. Acknowledgements

Authors would like to thank School of Mechanical Engineering, Universiti Sains Malaysia for providing the necessary financial support from FRGS grant No. 6070010.

6. References

1. Toda, M., Theory of Air Flow Generation by a Resonant Type PVF2Bimorph Cantilever Vibrator, Ferroelectrics, **22**, pp 911-918, 1979.
2. Yoo, J. H., Hong, J. I., and Cao, W., Piezoelectric Ceramic Bimorph Coupled to Thin Metal Plate as Cooling Fan for Electronic Devices," Sensors and Actuators A, **79**,pp 8-12, 2000.
3. Ro P I and Loh B G, Feasibility of using ultrasonic flexural waves as a cooling mechanism IEEE Trans. Indust.Electron. **48**, pp 143-150, 2001.
4. Tao Wu, Paul I Ro, Angus I K and James F M, Piezoelectric resonating structures for microelectronic cooling, **12**, Smart Mater. Struct., pp 181-187, 2003.
5. Buermann, P., Raman A., and Garimella, S. V., Dynamics and Topology Optimization of PiezoelectricFans, IEEE Transactions on Components and Packaging Technologies, **25**, pp 592-600, 2002.
6. W. Nakayama and S. H. Park, "Conjugate Heat Transfer from a Single Surface-Mounted Block to Forced Convective Air Flow in a Channel", Transactions of the ASME, Journal of Heat Transfer, **118**, pp. 301-309, 1996.
7. T. C. Hung and C. S. Fu, "Conjugate Heat Transfer Analysis for The Passive Enhancement of Electronic Cooling Through Geometric Modification in a Mixed Convection Domain", Numerical Heat Transfer, **35**, Part A, pp. 519-535, 1999.
8. G. A. Quadir, K. Y. Hung and K. N. Seetharamu, "A Computational Study of a PLCC Package In Mixed Convection," IJMEP, **23**, No.1, pp. 8-15, 2000.
9. Maram Venkata Ramana, K.N.Seetharamu, Indra Putra Almanar, Zaidi Mohd Ripin, "Some design Issues of Piezoelectric Resonating Structure for Cooling of Microelectronic Components", Proceedings of the 6th International Conference on Electronics Packaging Technology Conference, Singapore, pp264-269, 2004.

OPTIMIZATION OF PIEZOELECTRIC RESONATING STRUCTURE FOR COOLING OF MICROELECTRONIC COMPONENTS

BABBK
2795-7

Maram Venkata Ramana, K. N. Seetharamu[1], Indra Putra Almanar, Zaidi Mohd Ripin
School of Mechanical Engineering, University of Science Malaysia,
14300 Nibong Tebal , Penang , Malaysia.
[1]E-mail: knseetharamu@hotmail.com, fax: 060-4-5941025

Abstract: With the advancement of science and technology, electronic products have become faster and perform more functions. On the other hand, electronic products are also shrinking in size and weight. This will increase volumetric heat generation rates and surface heat fluxes in its components. As the size of electronic component reduces, cooling using a conventional fan may limit the miniaturization of these components. Therefore, it is important to develop a new cooling technology to improve performance of microelectronic components. This motivates the usage of Ultrasonic Flexural Wave (UFW) generated by a thin beam as a miniature fan. This can be achieved by using bimorph type bending actuator, which consists of two thin piezoelectric ceramic layers bonded together. Recent development in miniaturization of electronic components necessitates the optimal design of the resonator structures to generate the maximum cooling effect. The static, model and dynamic finite element analysis has been performed using cantilever piezoelectric bimorph to understand its mechanical behavior and to aid in design modifications. A three dimensional analysis was carried out by using commercial FEM software, ANSYS 6.0. In this paper, various parameters like length, thickness and location of the piezoelectric metal layer are used for investigation. The effects of these parameters on the vibration characteristics and performance merit are investigated and consolidated through Artificial Neural Network. Feedforward single hidden layer perceptron neural network and Levenberg-Marquardt backpropagation (LMBP) algorithm are used to train the neural network. Optimal geometrical conditions are then obtained using Genetic Algorithm.

INTRODUCTION

Piezoelectric bimorph structures are investigated as alternative cooling mechanism for cooling microelectronic components. Much research has been carried out experimental as well as numerical simulation[1]. The use of piezoelectric materials in sensors and actuators for actuating and controlling the smart structures were extensively studied by Luis and Crawly[2].The potential convective heat transfer capability of an UFW generated by direct and inverse piezoelectric effect was experimentally investigated by Ro.P.I and Loh B.G. [3,4].

There are several interesting aspects like length, thickness and location of the piezoceramic layer to perform at the optimum level. Considering the product of first ultrasonic resonance frequency to the corresponding dynamic tip-deflection as performance merit (PM).To achieve maximum cooling effect one have to maximize performance merit. This process involves solving static, model and harmonic simulations repeatedly. These analysis are complicated thus takes substantial amount of computer resources and require sound knowledge of working with ANSYS. Hence, In this work presents the applications of artificial neural network (ANN) and genetic algorithm(GA) approach to optimization of piezoelectric resonating bimorph structure. ANNs have been widely accepted as notable solution for modeling complex non-linear systems if the historical data is available. In recent years, ANN has been successfully applied in various fields such as control, finance, aerospace, manufacturing, electronics, industrial and manufacturing[5].

Most of the optimizations are carried out through numerical methods such as non-linear programming method and calculus based method. If the given function has more than one local maximum, optimization with these methods may produce the answer of local maximum instead of global maximum[6].Since these methods use principle of hill climbing by determination of gradients. This is where genetic algorithm (GA) come into picture. GA is a robust search tool based on natural evolution of genetics. Optimization with GA will always produce the global maximum of a given function. In this study GA used for the optimization of the piezoelectric resonating structure design .Azid et. al.[7]have applied GA for solving a number of truss problems with only support and load positions specified in terms of topology and geometric optimization. Jeevan et.al [8] have solved a PCB component placement problem using GA.

THEORY:

PIEZOELECTRIC FINITE ELEMENT FORMULATION:

Piezoelectric ceramics (piezoceramic) are solids that will generate a charge in response to the mechanical deformation, or it may be deformed mechanically when subjected to an electric field. Piezoelectricity is a coupled field effect. In piezoelectric material, stress and strain are coupled to electric field and polarization. Coupled-field elements are needed to perform piezoelectric analyses which contain all the necessary nodal degrees of freedom and include electrical–structural coupling in the element matrices.There are different principles used to develop the finite element equations which fit in the piezoelectric effect. The electromechanical constitutive behavior of a piezoelectric material within the linear scope can be shown in the following equations:

$$\{T\} = [c]\{S\} - [e]\{E\} \quad (1)$$

$$\{D\} = [e]^T\{S\} + [\varepsilon]\{E\} \quad (2)$$

where:

$\{T\}$ = stress vector

$\{D\}$ = electric flux density vector

$\{S\}$ = strain vector

$\{E\}$ = electric field vector

$[c]$ = elasticity stiffness matrix (evaluated at constant electric field)

$[e]$ = piezoelectric stress coefficient matrix

$[\varepsilon]$ = dielectric matrix (evaluated at constant strain)

Application of the variational principle of finite element discretisation to the coupled finite element discretisation yields the following equation can be expressed as

$$[M_{uu}]\{\ddot{u}\} + [C]\{\dot{u}\} + [K_{uu}]\{u\} + [K_{\varphi u}]\{\varphi\} = \{F\} \quad (3)$$

$$[K_{\varphi u}]\{u\} + [K_{\varphi\varphi}]\{\varphi\} = \{Q\} \quad (4)$$

where $[M_{uu}]$ and $[K_{uu}]$ are the mass and displacement stiffness matrices, $[K_{\varphi u}]$ is the piezoelectric coupling matrix, $[K_{\varphi\varphi}]$ is the dielectric stiffness matrix,[C] is the mechanical loss matrix and $\{F\}$ and $\{Q\}$ are respectively the mechanical force vector and the external applied electrical charge vector acting on the piezoelectric element.

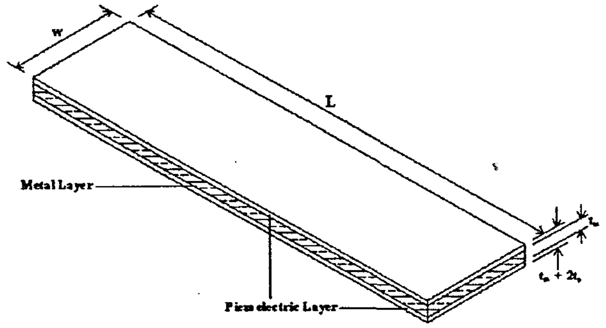

Fig. 1: Structure of Piezoelectric Bimorph

ANALYSIS

NUMERICAL SIMULATION METHOD

Static, modal and harmonic analysis, were performed in the numerical simulation by the commercial finite element method software package ANSYS . The effects of steady loading conditions on the piezoelectric structures are observed by conduction static analysis. Modal analysis is used to calculate the resonance frequencies and mode shapes of mechanical systems. When excited at or near it's resonance frequency, a resonator is most effective at converting energy. Modal analysis was carried by using the reduced method. The reduced method uses the HBI algorithm (Householder–bisection–inverse iteration) to calculate solution of the equation of motion of a deformable system. Reduced method with HBI algorithm is relatively fast because it uses the master DOF. In our simulation, the master DOF was chosen to be in the direction in which the beam vibrates. The full-method harmonic analysis was used to calculate the dynamic behavior of the structure, uses the full system matrices to calculate the harmonic response. To attain silent operation of resonator beam, operation frequency range was set over 20 kHz The bimorph is one of the most useful piezoelectric structures. It usually consists of two thin ceramic layers bonded together, which produces curvature when one ceramic layer expands while the other layer contracts. A center shim is usually laminated between the two piezoelectric layers to increase mechanical strength and stiffness, but reduces motion (Fig.1).To simulate the bimorph, the piezoelectric actuator patches were constructed using 3D coupled-field solid elements SOLID5 and the middle brass shim was modeled by SOLID45. The element edge lengths on surface boundaries of 0.5, 0.4, 0.3 and 0.2 mm were tested. Little variation in the parameters of

interest, i.e., resonance frequencies and dynamic displacements, was observed between the last two smallest grid solutions, so the final meshing edge length was 0.3 mm to guarantee reasonable accuracy and speed. The fixed–free boundary condition was applied by constraining the nodal displacements in *x, y* and *z* directions at one end of the beam. To simulate the electrode surfaces of the bimorph actuator, the same level of nodal electrical potential was prescribed at the nodes on the surfaces .

VERIFICATION OF NUMERICAL SIMULATION

Static and model analysis results are verified with analytical method for the model shown in figure1.As the bimorph (shown in figure 1) is made of metal and piezoceramic layer have different elastic moduli, transformed cross section method of composite beam selected to determine the static tip deflection and fundamental resonance frequency. The analytical expression for static tip deflection and fundamental resonance frequency are given in the following relations

$$\delta = \frac{3L^2}{2t}\frac{(1+B)(1+2B)}{AB^3+3B^2+3B+1}d_{31}E_3 \quad (5)$$

$$f_r = \frac{3.52t}{4\pi L^2}\sqrt{\frac{E_p}{3\rho_p}}\left[\frac{1+3(1+2B)^2+4AB^3}{4(1+B)^2(BC+1)}\right]^{1/2} \quad (6)$$

where:

δ = static tip deflection

f_r = fundamental resonance frequency

d_{31} = piezoelectric constant

E_3 = electric field strength

E_m = Young's modulus of metal

E_p = Young's modulus of piezoelectric layer

ρ_m = density of metal

ρ_p = density of piezoelectric layer

t_m = thickness of metal

t_p = thickness of piezoelectric

L = length of the beam

t = total thickness of the bimorph $= t_m + 2t_p$

$$A = \frac{E_m}{E_p}, \quad B = \frac{t_m}{2t_p}, \quad C = \frac{\rho_m}{\rho_p}$$

A bimorph of an 8 mm × 2 mm metal shim bonded with two same-size ceramic layers was used to compare numerical simulation results with the analytical ones that are obtained using equations (5) and (6). The properties of PZT ceramic and two alternative metal materials are listed in table 1.The static response of the bimorph was determined by applying an electrical field of 200 V mm−1 on both PZT patches. Keeping the total thickness constant at *t* = 0.4 mm,

Table 1. Material properties.

Materials	*d*31	Young's Modulus ($\times 10^{10}$ N m^{-2})	Density (kg m^{-3})	Poisson 's ratio
PZT ceramic	190 × 10^{-12}	6.6	7800	0.31
PZT 5A	-171	6.1	7750	0.35
Brass	--	11	8800	0.35
Alumni.	--	6.5	2992	0.35

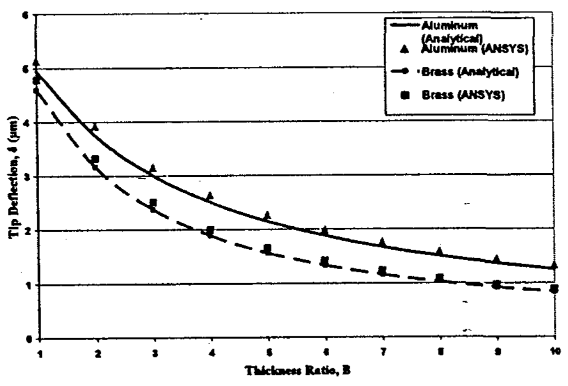

Fig. 2: Static Tip Deflection Vs Thickness Ratio.

The effect of an elastic layer on tip deflection can be obtained by plotting tip deflection δ versus thickness ratio B for two elastic materials, as shown in Fig. 2. As the metal layer thickness increases and the PZT layer decreases (B increases), tip deflection will decrease, and more quickly so for a stiffer metal layer. The result obtained by the analytical approach is included for comparison. Good agreement is shown for the results obtained from the analysis and simulation using the finite element method.

Modal analysis is used to obtain the mode shapes. Fundamental resonance frequency *fr* versus thickness ratio *B* for brass and aluminum

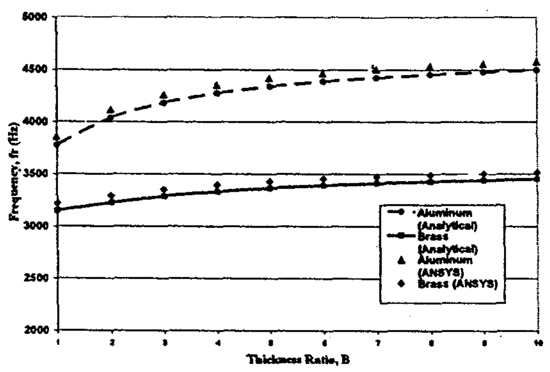

Fig. 3: Resonance Frequency Vs Thickness Ratio.

is shown in Fig. 3. It can be seen that the use of an aluminum metal layer leads to much higher resonance frequency than brass because of its lower density. Comparing the simulation results with analytical ones, the difference is within 10%. The good agreement between the finite element simulation and the analytical solution gives confidence that the present computer simulation method is sufficiently accurate to analyze more complicated piezoelectric structures.

OPTIMIZATION OF PIEZOELECTRIC STRUCTURE DESIGN

In the resonator structure design, bimorph is excited at the ultrasonic frequency range to take the advantage of the acoustic streaming. Acoustic streaming is a steady circular airflow occurring in a high-intensity sound field which can increase the convective heat transfer rate []. The acoustic streaming velocity is proportional to the product of the frequency and displacement amplitude of the vibration wave. From the modal analyses, it is found that, for the cantilevers, the maximum displacement occurs at the tip. So the product of natural frequency f and dynamic tip deflection A is chosen to be a performance merit to evaluate the cooling effect by the piezoelectric structure.

$$P.M = f * A. \qquad (11)$$

In our simulation, bimorph is made of two-layer piezoceramic (PZT 5A) reinforced with center brass layer. The thickness of the brass shim is 0.127 mm and the thickness for each of two ceramic sheets is 0.191 mm which brings the total thickness of the bimorph to 0.508 mm. The material properties of the PZT 5A and brass are shown in the table 1. In modal analysis, Ten modes were extracted and expanded, among which the first mode of vibration in the ultrasonic range was selected. In harmonic analysis, the electric field of alternating voltage 20 V cm−1 was applied on both ceramics. A constant damping ratio of 1% was assumed over all frequencies of the harmonic analysis range. Four different piezoelectric models were simulated as follows:

Table 3.Bimorph configurations

Case	Length (L) cm	Length of Patch(LP)	Center of patch(CP)
1	1.0,0.8,0.6	L = LP	L/2
2	0.8	0.1 to 0.7	3.5
3	0.8	0.1 to 0.7	4.5

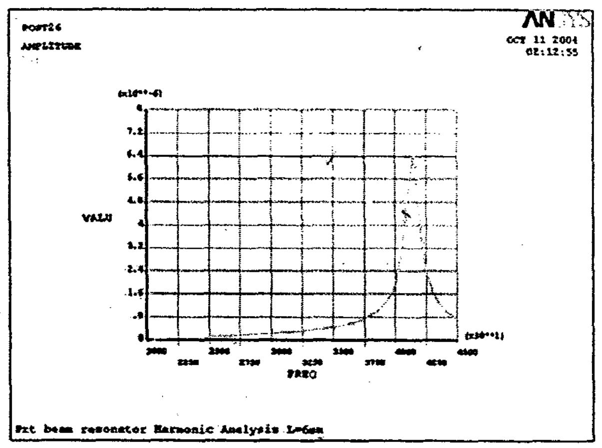

Fig. 4:Amplitude of bimorph, L =0.6cm

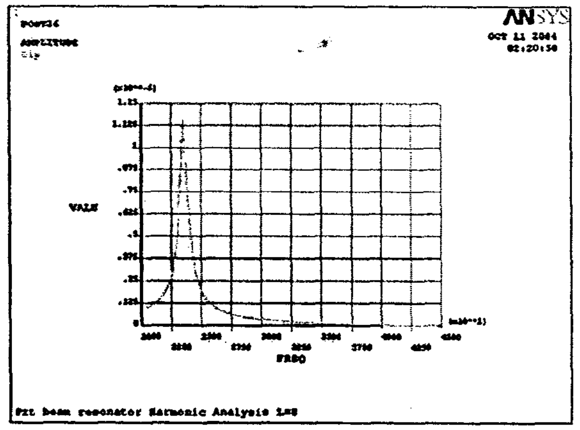

Fig. 5:Amplitude of bimorph, L =0.8cm

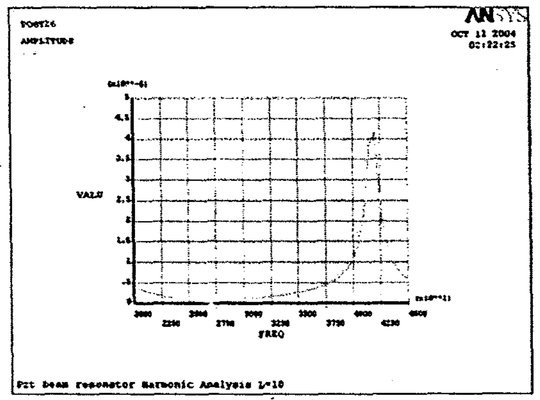

Fig. 6:Amplitude of bimorph, L =1.0cm

Table 4. Comparative performance merit

Bimorph Length (cm)	First ultrasonic resonance frequency	Tip amplitude (μm)	Performance Merit
0.6	42231	6.38	1.6936
0.8	24005	1.16	1.7533
1.0	45626	4.27	1.2242

APPLICATION OF ANN AND GA

Artificial Neural Network is applied to investigate the parameter of interest. The ANN method applied in this paper consists of single hidden layer with 10 neurons using *Neural Network Toolbox* of MATLAB 6.5. ANN is trained to learn the behavior of performance merit which is a product of the first ultrasonic resonance frequency to dynamic tip-deflection. The input and output to the ANN is length ratio(LR) and performance merit respectively. After ANN trained, intermediate values of performance merit predicted for the configurations Case 2 and Case 3 and are presented in Fig.7 and Fig.8 respectively.

GA is used to optimize the performance merit . The output of the ANN is used as input to GA. The optimum configurations predicted by GA is listed in Table5.

CONCLUTIONS

This paper presents the successful application of artificial neural network and Genetic Algorithm in the optimization of the piezoelectric resonating structure. It is shown that ANN could be used as useful tool for prediction whenever the historical data is available. ANNs can be used in various optimization applications in cases where modeling and numerical solutions are complex and tactful to be done. As seen from the table 5 optimization with GA will always produce the global maximum of a given function.

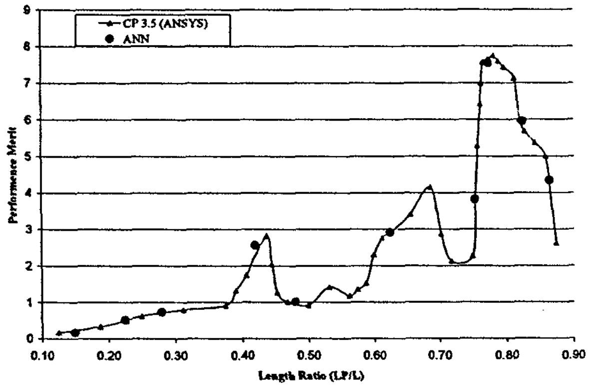

Fig. 7:Case2 Ann predictions with Ansys input data

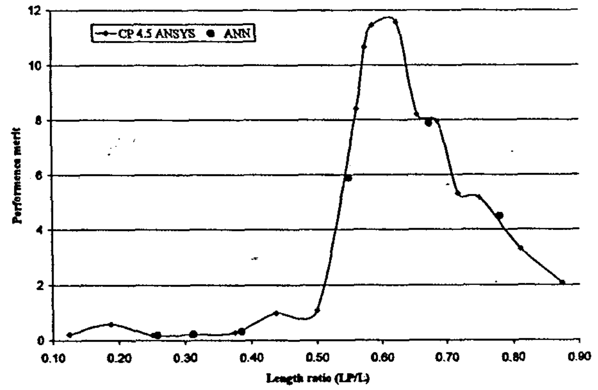

Fig. 8:Case3 Ann predictions with Ansys input data

Table 5. Optimum values from genetic Algorithm

Case	Length ratio (LP/L)	Length of Patch(LP)
CP=3.5	0.782	7.742
CP=4.5	0.623	11.753

REFERENCES

1. Ro P I and Loh B G, "Feasibility of Using Flexural Waves as a Cooling Mechanism", *IEEE Transactions on Industrial Electronics*, Vol.48, No.1, pp 143-149. February, 2001
2. Crawly E F and Luis D J, "Use of Piezoelectric Actuator as Elements of Intelligent Structures", *AIAA J.25*, Pages 1373-1385, 1987
3. Tao Wu, Paul I Ro, Angus I Kingon and James F Mulling, "Piezoelectric Resonating Structures for Microelectronic Cooling", *Institute of Physics Publishing, Smart Materials and Structures*, 12 , pages 181-187,2003.
4. Loh B G, Hyun S, Ro P I and Kleinstreuer C, "Acoustic Streaming Induced by Ultrasonic Flexural Vibrations and Associated Enhancement of convective heat transfer" *J. Acoust. Soc. Am.*, 111, 875-883,2002
5. Aratti R.B, Cannas B Fanni A , Pintus M, Sechi G M, Toreno N, "River flow forecast for reservoir management through neural networks" *Int Comm. Neurocomputing* Vol. 55, Elsevier Science Ltd. pp421-437, 2003
6. David E. Goldberg, Genetic Algorithms in search, Optimization, and Machine Learning, Addison Wesley,1989.
7. Azid I.A,A.S.K. Kwan and K.N.Seetharamu, "A GA based technique for layout optimization of Trusswith stress and displacement constranints,I.J.Num.Meth.In.Engineering,Volume 53,1641-1674,2002
8. K.Jeevan,A.parthiban,K.N.Seetharamu " Optimization of PCB Component Placement Using Genetic Algorithms,Journal of Electronics Manufacturings,Vol 11,No 4,69-79,2002
9. C S Krishnamoorthy, Indian Institute of Technology, Madras, *Finite Element Analysis, Theory and Programming*, Tata McGraw-Hill Publishing Company Limited, New Delhi,1987
10. Lin M W and Abatan A O "Application of commercial finite element codes for the analysis of induced strain-actuated structures" J.Intell. Mater. Syst.Struc.5,869-875,1994.
11. *ANSYS 7.0 Documentation* (ANSYS Help Files).

PIEZO SYSTEMS, INC.
186 Massachusetts Avenue Cambridge, MA 02139 • Tel: (617) 547-1777 • Fax: (617) 354-2200 • Web: www.piezo.com • E-mail: sales@piezo.com

LOW VOLTAGE PIEZO FAN BLADE
12 - 24VDC / 125 Hz VERSION

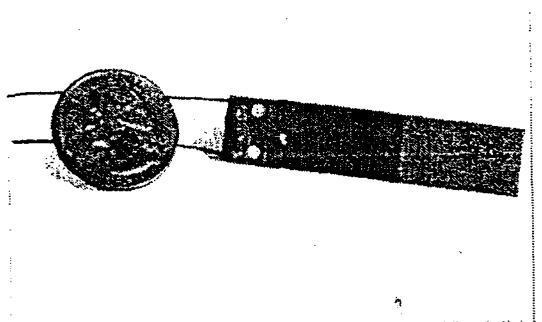

ITEM	PART NO.
Low Voltage Piezo Fan	RFN1-LV1

The low voltage piezo fan is a solid state device designed to be used where low DC input voltage (12 - 24 VDC) is available. The fan comprises a compound piezo/stainless steel blade mounted to a PCB mount incorporating a filter and bleed resistor. Oscillating blade motion creates a high velocity flow stream emanating from the leading edge of the blade. Air intake is above and below the swept out volume of the blade.

Piezo fans offer the following advantages: instant starting with no power surge (especially desirable for spot cooling); ultralight weight; thin profile; no EMI; high reliability; operation over a wide temperature range; and almost no heat dissipation (ideal for sealed enclosures).

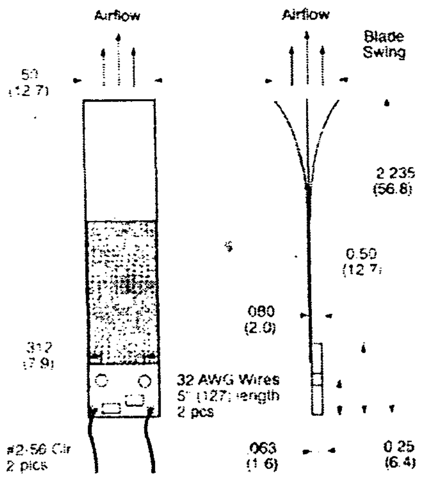

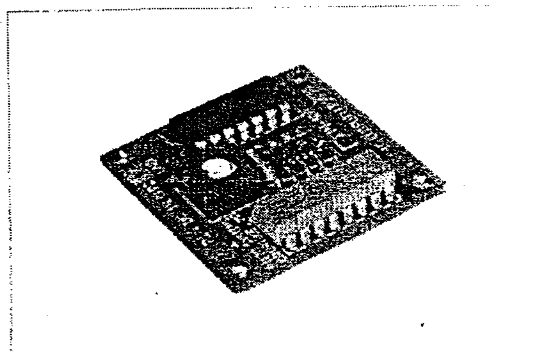

ITEM	PART NO.
Inverter Drive Circuit	EIN-407

An inverter circuit converts a DC input voltage to an oscillating AC output voltage. Piezo System's Inverter Drive circuit provides a low voltage (up to ±44 Vp), low frequency (50 Hz - 150 Hz) signal for driving resonant piezo devices such as fans, choppers, and vibrators. Output frequency is adjusted manually by turning the trimmer pot on the PCB. Optimum tuning is accomplished by visual observation of the device motion or inspection of the output waveform on an oscilloscope during operation.

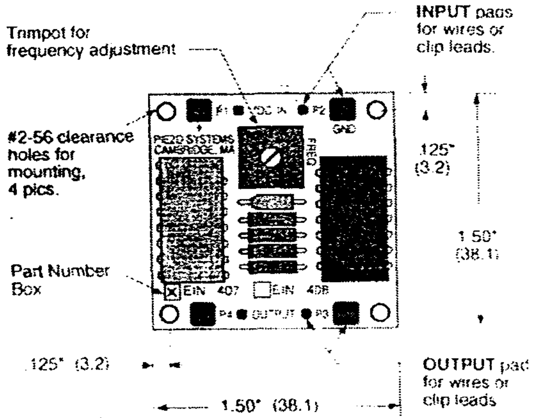

LOW VOLTAGE
PIEZO FAN KIT

PIEZO SYSTEMS, INC.
186 Massachusetts Avenue Cambridge, MA 02139 • Tel: (617) 547-1777 • Fax: (617) 354-2200 • Web: www.piezo.com • E-mail: sales@piezo.com

SET-UP INSTRUCTIONS

Powering and wiring the fan using the Inverter Drive Circuit: A DC power supply (either variable or fixed) up to 24 VDC is required. With the power turned off and the voltage turned down, attach the positive lead from the DC power supply to the positive pad (P1) of the Inverter Drive Circuit input. Attach the negative lead from the DC supply to the ground pad (P2) of the Inverter Drive Circuit input. If the leads are reversed, the inverter circuit may be damaged.

Attach the leads from the piezo fan to the output pads (P3 and P4) from the Inverter Drive Circuit. Turn on the DC power supply and adjust the voltage level to the desired setting. The inverter continually "flips" the polarity of the output terminals to obtain the peak-to-peak output voltage.

Adjusting the drive voltage: The low voltage piezo fan is rated up to ±24 volts peak. It is possible to drive the fan to higher voltages (since the Inverter Circuit is rated to ±44 volts peak). Driving the fan beyond ±24 volts peak may result in overstraining the fan blade since it is a resonating structure. User discretion is advised.

Adjusting the drive frequency: Using a small screwdriver, adjust the trimpot to produce maximum fan blade amplitude. This occurs when the inverter circuit delivers a signal frequency which corresponds to the fan's natural frequency. Be aware that the resonant frequency can shift slightly with increasing voltage.

Note: Since piezoceramic is pyroelectric as well as piezoelectric, it generates a voltage proportional to a temperature change (assuming no charge leakage). The polarity of the voltage is positive when the temperature increases, and negative when the temperature decreases. A sufficiently large drop in temperature can produce a depoling voltage if the charge can not leak away. For this reason, the inverter circuit has a bleed resistor across the output terminals. If the fan is not connected to the circuit it is good practice to short the leads together for storage.

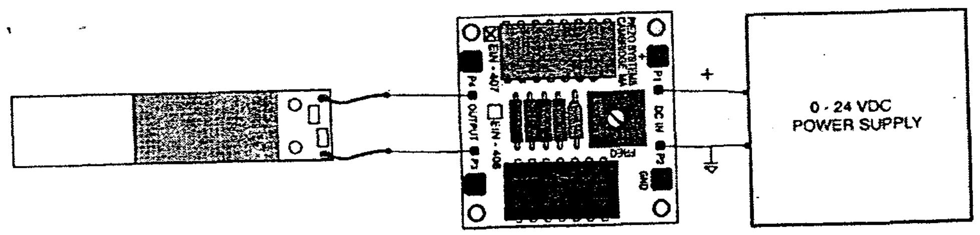

LOW VOLTAGE PIEZO FAN KIT

PIEZO SYSTEMS, INC.
186 Massachusetts Avenue Cambridge, MA 02139 • Tel: (617) 547-1777 • Fax: (617) 354-2200 • Web: www.piezo.com • E-mail: sales@piezo.com

LOW VOLTAGE PIEZO FAN SPECIFICATIONS

Input Voltage to Inverter Drive Circuit:	VDC	12 VDC	15 VDC	24 VDC
Current drawn by fan and circuit:	mA	1.0	1.5	2.7
Power Consumption of fan and circuit:	mW	12	22.5	65
Volume Flow Rate:	CFM (l/s)	0.25 (.12)	0.40 (.19)	0.75 (.35)
Peak Air Velocity:	FPM (m/s)	235 (1.2)	315 (1.6)	435(2.2)
Resonant Frequency:	Hz	125	125	125
Blade Swing, peak to peak:	inches (mm)	0.24 (6.1)	0.27 (6.9)	0.37 (9.4)
Fan Capacitance	nF		45	
Fan Weight	grams		2.0	
Fan Temperature Range:	°C		-40° to 90°	

INVERTER DRIVE CIRCUIT SPECIFICATIONS

		EIN-407
Input Voltage Range	VDC	0 to 44
Output Voltage Range	Vp	0 to ± 44
Frequency Range	Hz	50 - 150
Temperature Range	°C	0 -60
Weight	grams	8

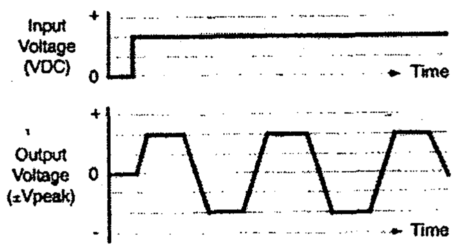

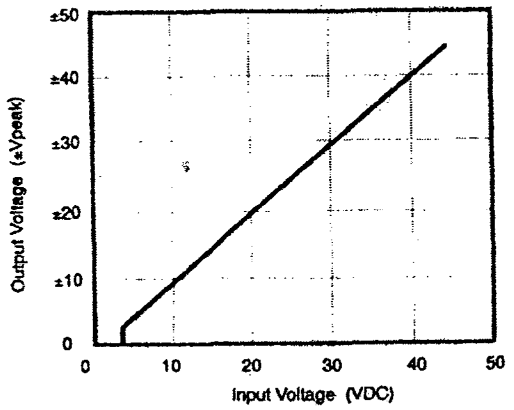

ELECTRONICS

PIEZO SYSTEMS, INC.
186 Massachusetts Avenue Cambridge, MA 02139 • Phone: (617) 547-1777 • Fax: (617) 354-2200 • Web: www.piezo.com • E-mail: sales@piezo.com

DC TO AC INVERTER DRIVE CIRCUIT

MEASURING INVERTER OUTPUT

The inverter circuit continually "flips" the polarity of the output terminals to obtain the peak-to-peak output voltage. Because of this, you can not ground either of the output terminals without shorting half of the output signal. If you want to see the output signal, do one of the following:

1. To see the peak output voltage and frequency (the actual output voltage will be 2X what is seen on the scope).
   - Connect the scope ground to terminal P2 (DC IN - GND):
   - Connect the scope probe to either output terminal (P3 or P4).
   - Figure-1 shows the scope trace you should see with a 2 channel scope.

2. To see the full output voltage and frequency between P3 and P4 (a 2 channel differential scope is required):
   - Connect the scope ground to terminal P2 (DC IN - GND).
   - Connect Channel-1 to P3.
   - Connect Channel-2 to P4.
   - Set scope for differential measurement (Channel 1 - Channel 2).
   - Figure-2 shows the scope trace you should see with a 2 channel differential scope.

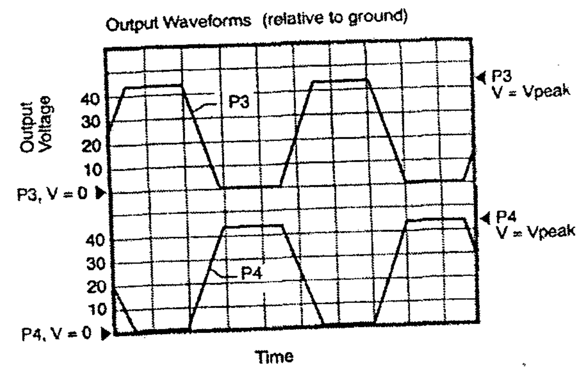

Figure-1. Peak Output Voltage versus Time Between Terminal P3 or P4 and Ground.

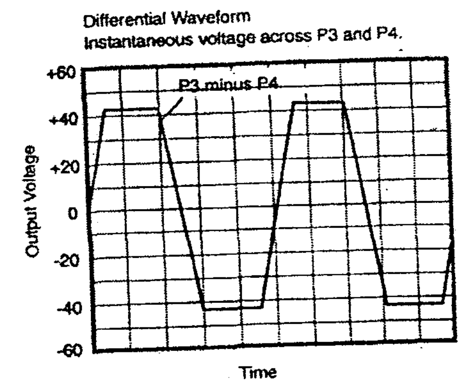

Figure-2. Peak-to-Peak Output Voltage versus Time Across Terminals P3 and P4